A Comparison of Sampling Methods for a Standing Tree Acoustic Device

Jerry M. Mahon Jr., Lewis Jordan, Laurence R. Schimleck, Alexander Clark III, and Richard F. Daniels

ABSTRACT

One method of evaluating potential product performance is the use of acoustic tools for identifying trees with high stiffness. Acoustic velocities for 100 standing loblolly pine (*Pinus taeda*) trees, obtained with the transmitting and receiving probes placed on the same face and opposite faces, were compared. Significant differences in velocity between the two methods were found, with velocity determined using the opposite-face method generally dependent on stem diameter, or the amount of wood through which the stress wave must pass. The only opposite-face method in which the velocities did not vary with dbh was for an assumed flight path where the stress wave traveled from the transmitting probe around the circumference of the stem in the outerwood and then down longitudinally to the receiving probe. Variation in velocities from hit-to-hit was 62% less using the opposite-face method compared with the same-face method. It is recommended to use the circumferential opposite-face (Vel_OC) calculation when determining stress wave velocity for a standing tree.

Keywords: acoustic velocity, analysis of covariance, loblolly pine, time of flight, TreeSonic

When southern pine dimension lumber is visually graded, it is given a grade that has assigned strength and stiffness design values. Young fast-growing trees may not have the stiffness required to make no. 2 lumber. Thus, there is an ever-increasing need to segregate standing trees or lumber based on certain wood properties or mechanical performance. Early determination of tree stiffness will not only help identify the best end use of the resource, but will also maximize revenue (Matheson et al. 2002). Although mills are not currently rewarding landowners that grow trees with high stiffness, an acoustic device could aid the procurement process by identifying wood baskets with desirable wood properties. This would provide sawmills, both producing machine stress graded and visually graded lumber, the ability to increase their profits by purchasing raw material that could have a higher proportion of no. 1 and 2 grade lumber. Recently, acoustic tools have been examined as a rapid, nondestructive method for identifying trees with high stiffness or modulus of elasticity (MOE) and is increasingly being used within the forest industry (Lindstrom et al. 2002; Matheson et al. 2002; Wang et al. 2001, 2007; Grabianowski et al. 2006; Toulmin and Raymond 2007).

Acoustic devices generally consist of a transmitting probe, which induces a stress wave that travels through the stem and is detected by a receiving probe, located at a known distance from the transmitter. The time it takes for the stress wave to travel from the transmitter to the receiver is recorded and is known as the time of flight (TOF). For known distance (d), the velocity (v), or the rate of propagation through the material, is simply distance divided by TOF ($v = d/\text{TOF}$). If the green density (ρ) of the material is known, the dynamic MOE then can be calculated as ρ multiplied by velocity squared ($\text{MOE} = \rho v^2$). Thus, acoustic tools can provide a rapid, nondestructive measure of MOE, the standard for which solidwood products are judged, and are of enormous benefit to the forest products industry.

Numerous authors report strong relationships between stress wave and machine graded MOE (Wang et al. 2001, Matheson et al. 2002, Joe et al. 2004). Wang et al. (2001) reports statistically significant relationships between stress wave–determined MOE and static MOE of lumber cut from logs with R^2 values ranging from 0.44 to 0.89. Similar results were observed by Matheson et al. (2002) when examining the relationship between cut boards and stress wave velocity in logs of radiata pine (*Pinus radiata*; $R = 0.50$). Joe et al. (2004), when examining the relationship between whole log stress wave velocity and machine graded MOE in *Eucalyptus dunnii*, found correlations of 0.72 and 0.73 for trees 9 and 25 years old, respectively.

These findings verify the usefulness of acoustics for estimating log and lumber stiffness. However, for practical purposes, evaluation of standing tree stiffness within a plantation, before or at the time of harvest, is a desirable goal, because it would prevent the present redundancy of sorting high and low stiffness logs after delivery to a suitable market. Recently, Carter and Sharplen (2006) filed a patent for a timber harvesting apparatus that implements an acoustic device in a harvester head. The purpose of the modified

Received January 9, 2008; accepted April 3, 2008.

Jerry M. Mahon Jr. (jmahon@molpus.com). Lewis Jordan (lewis.jordan@weyerhaeuser.com), Weyerhaeuser Company, Columbus, MS 39701. Laurence R. Schimleck (lschimleck@warnell.uga.edu), Warnell School of Forestry and Natural Resources, The University of Georgia, Athens, GA 30602. Alexander Clark III (aclark@fs.fed.us), US Forest Service (retired), Southern Research Station, Athens, GA 30602. Richard F. Daniels (ddaniels@warnell.uga.edu), Warnell School of Forestry and Natural Resources, The University of Georgia, Athens, GA 30602. *The authors acknowledge the support from the sponsors of the Wood Quality Consortium of The University of Georgia and the US Forest Service. Thanks are also extended to Dr. Xiping Wang and the three anonymous reviewers for their helpful comments. This article is based on the first author's Masters research at The University of Georgia.*

This article uses metric units; the applicable conversion factors are: centimeters (cm): 1 cm = 0.39 in.; meters (m): 1 m = 3.3 ft; hectares (ha): 1 ha = 2.47 ac.

harvester head is to properly sort felled trees/logs at the logging deck before delivery to the desired market.

Questions have been raised regarding costs associated with the implementation of acoustic devices. It is unclear whether the landowners' revenue would be decreased because of an increased logging cost associated with the implementation of an acoustic device on a harvester head or if the landowner's revenue would be increased because of increased stumpage rates for high stiffness trees. These are important concerns acoustic researchers must address, but if significant relationships can be established between standing/felled tree stress wave–determined TOF, velocity, or MOE values and individual tree characteristics, then this would allow for maximum efficiency in the sorting process.

Matheson et al. (2002) found mixed results when correlating standing tree stress wave velocity and lumber cut from logs in radiata pine, reporting correlations of $R = 0.33$ (control seedlot) and $R = 0.01$ (orchard lot). Joe et al. (2004) also reported significant relationships between standing tree acoustics and machine graded MOE with correlations of $R = 0.40$ and $R = 0.44$ in *E. dunnii*. These findings clearly show low correlations between standing tree acoustic velocity and stress graded lumber taken from the whole stem. In a recent study, however, Grabianowski et al. (2006) reported standing tree acoustic velocities correlated well with lumber cut both adjacent to the bark and corewood with R^2 values of 0.89 and 0.74, respectively. The significance of dbh on the relationship between acoustic velocity, stress wave–determined MOE and machine graded MOE has also been investigated. Joe et al. (2004) found no significant relationships when correlating dbh with acoustic velocity and machine graded MOE values, while Toulmin and Raymond (2007) reported minimal relationships between dbh and acoustic velocities in radiata pine with R^2 values of 0.07, 0.09, and 0.04 for stands aged 10, 15, and 20 years, respectively. Similar findings were reported by Chauhan and Walker (2006) when examining the relationship between acoustic velocity, outerwood density, and dbh in radiata pine stands aged 8, 16, and 25 years. Chauhan and Walker (2006) reported R^2 values of 0.02, 0.07, and 0.18 at 8, 16, and 25 years respectively, when regressing velocity on outerwood density. They also found poor relationships between velocity and dbh with R^2 values of 0.18, 0.06, and 0.14 at 8, 16, and 25 years, respectively.

In the current literature, for evaluating standing tree acoustics, there are two general methods of measurement: (i) the transmitting and receiving probes are placed on the same face of the tree at some prespecified distance (generally 1 m; Lindstrom et al. 2002, Wang et al. 2001, Grabianowski et al. 2006) and (ii) the transmitting and receiving probes are placed on opposite faces of the tree at some prespecified distance (generally 1 m; Matheson et al. 2002, Joe et al. 2004; Figure 1). Once velocities have been recorded, researchers have then attempted to correlate standing tree stress wave–determined TOF, velocity, or MOE values with observed averaged machine graded MOE from cut boards, green density, or tree characteristics such as dbh.

Matheson et al. (2002) conjectures that the induced stress wave "may travel through the heart of the tree (where flight time is expected to be least) or may travel around the tree in the stiffer sapwood (where the flight time is expected to be greatest)," when using the opposite-face method. For TOF, or velocity, determined using the same-face method, it is hypothesized that the stress wave travels longitudinally in the wood between the transmitting and receiving probes. However, no research has been done to compare the differences in velocities obtained using the same- and opposite-face methods. This has implications when trying to correlate stress wave–determined TOF, velocity, or MOE values with observed averaged machine graded MOE from cut boards, green density, or tree characteristics.

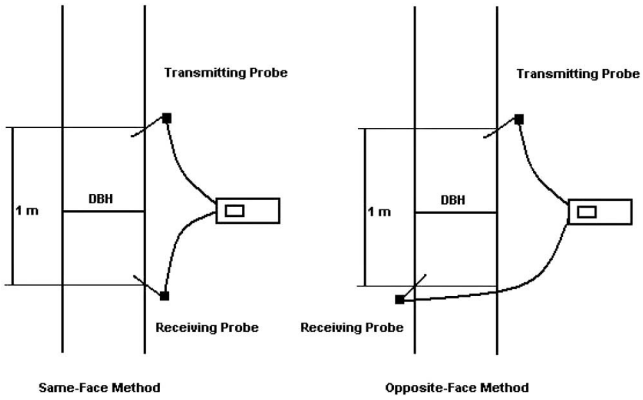

Figure 1. Experimental setup to compare same-face and opposite-face methods.

The objective of this work was to examine differences in acoustic velocities using the FAKOPP TreeSonic microsecond timer device when the probes are placed on the same face and the opposite face and to explore possible flight paths for stress waves through standing trees. This is accomplished by calculating velocities that are adjusted by the distance the stress wave travels under six different hypothesized flight paths.

Materials and Methods

One hundred loblolly pine trees were sampled from a research plot established in 1989 by the Consortium for Accelerated Pine Production Studies of the University of Georgia in Clarke County, Georgia. The research plot, approximately 0.4 ha, was intensively managed, and the treatments were described by Borders et al. (2004). Candidate trees were selected based on desirable sawing properties (straightness, small branching, etc.). The trees selected for sampling represented the diameter distribution of the candidate trees and ranged in dbh from 16.8 to 35.8 cm and averaged 25.4 cm. Total height of the sample trees ranged from 17.5 to 26.4 m and averaged 22.1 m.

The FAKOPP TreeSonic device is an acoustic tool designed to measure standing trees (Booker and Ridoutt 1997, Lindstrom et al. 2002). The FAKOPP TreeSonic is comprised of two probes, a transmitting accelerometer and a receiving accelerometer. For measurements on standing trees it is recommended that the probes are placed 1 m apart. FAKKOP's TreeSonic was used to measure the TOF (meters per second) between the transmitting and receiving probes for all 100 trees, from which velocity was calculated. For the same-face method, the probes were positioned 1 m apart and centered on dbh. For the opposite-face method, the transmitting probe was placed 0.5 m above dbh on one face of the tree; the receiving probe was then placed on the opposite face 0.5 m below dbh such that the distance between the transmitting and receiving probes was 1 m (Figure 1). To ensure an accurate estimate, both methods were applied on the four cardinal faces of each sample tree, with each face receiving 5 hits, for a total of 20 velocities for each method, respectively.

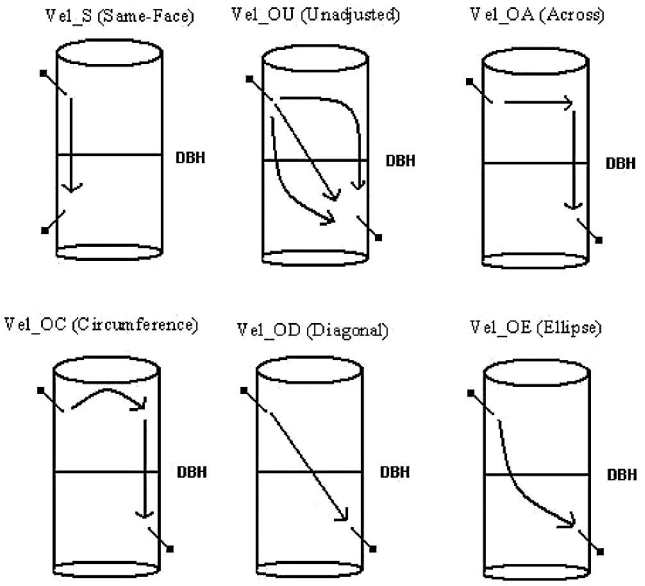

Figure 2. Hypothesized stress wave flight paths for the same-face and distance adjusted values.

Researchers using the opposite-face method, generally, assume that the distance the stress wave travels through the standing tree is 1 m, because this is generally how far apart the probes are placed on the tree (Figure 1). This is not an unreasonable assumption using the same-face method, but it fails to take into account the amount of wood through which the stress wave must pass when using the opposite-face method and would lead to underestimated acoustic velocities for larger trees. One alternative is to use a covariate such as dbh to adjust the velocities. However, by calculating the distance between the transmitting and receiving probes using hypothesized flight paths, one can then adjust the velocities accordingly, potentially removing the effect of the amount of wood through which the stress wave passes.

Flight Paths

We propose six flight paths, which the stress wave could take within the stem, leading to six unique acoustic velocities (Figure 2). These velocities are defined as

i. Vel_S = the same-face method: Assuming the flight path of the stress wave from the transmitting probe travels longitudinally down the wood a distance of 1 m to the receiving probe.
ii. Vel_OU = the unadjusted opposite-face method: Assuming a distance of 1 m, the flight path of the stress wave is considered unknown and could travel in any direction through the stem.
iii. Vel_OA = the across adjusted opposite-face method. Assuming the flight path from the transmitting probe has an initial direction traveling radially through the center of the stem and down 1 m to the receiving probe.
iv. Vel_OC = the circumference adjusted opposite-face method: Assuming the flight path from the transmitting probe has an initial direction traveling circumferentially around the stem in the outerwood and down 1 m to the receiving probe.
v. Vel_OD = the diagonally adjusted opposite-face method: Assuming the flight from the transmitting probe travels in a straight line to the receiving probe, passing through the heart of the tree.
vi. Vel_OE = the ellipse adjusted opposite-face method: Assuming the flight path from the transmitting probe has an initial direction traveling the shortest distance between the transmitting and receiving probes elliptically through the outerwood across the stem to the receiving probe.

For simplicity, we assumed the 1-m section of the stem between the transmitting and receiving probes was a cylinder, with diameter equal to dbh. The method of calculating the six acoustic velocities are given as

$$\text{Vel\_S} = 1/\text{TOF} \quad (1)$$

$$\text{Vel\_OU} = 1/\text{TOF} \quad (2)$$

$$\text{Vel\_OA} = [(\text{dbh}/100) + 1]/\text{TOF} \quad (3)$$

$$\text{Vel\_OC} = [(C/2) + 1]/\text{TOF} \quad (4)$$

$$\text{Vel\_OD} = [\sqrt{1^2 + (\text{dbh}/100)^2}]/\text{TOF} \quad (5)$$

$$\text{Vel\_OE} = D^*/\text{TOF} \quad (6)$$

where, $C = (\text{dbh}\pi)/100$ is the circumference of the stem in meters, $D^* = \{\pi(a + b)[1 + 3h/(10 + \sqrt{4 - 3h})]\}/2$ (one-half the circumference of an ellipse), $a = \sqrt{1^2 + (\text{dbh}/100)^2}$, $b = (\text{dbh}/100)/2$, and $h = (a - b)^2/(a + b)^2$. D^* was calculated using Ramanujan's second approximation for the circumference of an ellipse.

The distance and corresponding adjusted velocities for each hypothesized flight path can be calculated using the foregoing equations (Table 1). The average velocities for each method were found to range from 3,092.16 to 4,312.25. The distance of the flight path for the Vel_S and Vel_OU methods was held constant at 1 m, and thus averaged 1 m. The average distance of the flight path for Vel_OA, Vel_OC, Vel_OD, and Vel_OE was found to be 1.25, 1.40, 1.03, and 1.11 m, respectively. For the duration of this analysis, we refer to Vel_S as the same-face method, and Vel_OU, Vel_OA, Vel_OC, Vel_OD, Vel_OE, as the opposite-face method.

Statistical Analysis

The experimental design for this study constitutes a randomized complete block design with subsampling. Each sample tree corresponds to a block, the treatment consisting of the method used in calculating velocity (Vel_S, Vel_OU, Vel_OA, Vel_OC, Vel_OD, and Vel_OE), and the multiple hits corresponding to the subsample. The general form of this model can be expressed as

$$y_{ijk} = \mu + \text{M}_i + t_j + (\text{Mt})_{ij} + e_{ijk}, \quad (7)$$

where y_{ijk} is the velocity of the kth hit of the jth tree with the ith method (i = Vel_S, Vel_OU, Vel_OA, Vel_OC, Vel_OD, and

Table 1. Average and range (in parenthesis) of velocities and distances for each hypothesized flight path.

Method	Velocity (m/s)	Distance (m)
Vel_S (same-face)	3821.77 (2604.17–4651.16)	1.00 (1.00–1.00)
Vel_OU (unadjusted)	3092.16 (2487.56–4098.36)	1.00 (1.00–1.00)
Vel_OA (across)	3868.89 (3030.73–4899.92)	1.25 (1.17–1.36)
Vel_OC (circumference)	4312.25 (3332.89–5357.44)	1.40 (1.26–1.56)
Vel_OD (diagonal)	3191.37 (2570.37–4176.01)	1.03 (1.01–1.06)
Vel_OE (elliptical)	3415.32 (2699.26–4373.28)	1.11 (1.05–1.19)

Vel_OE and $j = 1, \ldots, 100$ and $k = 1, \ldots, 20$); μ is the population mean; M_i is the effect of the ith method; t_j is the random effect of the jth tree, with $t_j \sim N(0, \sigma^2_t)$; $(Mt)_{ij}$ is the random interaction effect between the ith method and jth tree, with $(Mt)_{ij} \sim N(0, \sigma^2_{Mt})$; and e_{ijk} is residual error with $e_{ijk} \sim N(0, \sigma^2)$.

Although fairly general, Equation 7 does not account for the variability in the trees that could not be controlled by the experimental design. In addition to the response variable (velocity), all trees were measured for dbh. An analysis of covariance was performed using dbh as a covariate and the full model can be written as

$$y_{ijk} = \beta_0 + \beta_{0i} + \beta_1 DBH_{ij} + \beta_{1i} DBH_{ij} + t_j + (Mt)_{ij} + e_{ijk}, \quad (8)$$

where β_0 and β_1 are the population intercept and slope regression coefficients, respectively; β_{0i} and β_{1i} are the treatment effect coefficients; and all other variables are as previously defined. Equation 8 was fit to compare the velocities calculated using the assumed flight paths. The models in this article were fit using the SAS MIXED procedure, with Satterthwaite's approximation for computing the denominator degrees of freedom for the fixed effects (SAS Institute, Inc., 2004).

Results

We fit the full model, Equation 8, to test the hypothesis that all slopes are equal to zero; $H_o : \beta_{1,Vel\_S} = \beta_{1,Vel\_OU} = \beta_{1,Vel\_OA} = \beta_{1,Vel\_OC} = \beta_{1,Vel\_OD} = \beta_{1,Vel\_OE} = 0$ versus H_a : (not H_o :). The $F_{6,292}$ value and P-value of this test were 75.78 and 0.0001, respectively. We rejected H_o and concluded that the slopes are most likely not all equal to zero. We then tested the hypothesis $H_o : \beta_{1,Vel\_S} = \beta_{1,Vel\_OU} = \beta_{1,Vel\_OA} = \beta_{1,Vel\_OC} = \beta_{1,Vel\_OD} = \beta_{1,Vel\_OE} = \beta$, to determine if a common slope model would be adequate to describe the data. The $F_{5,491}$ value and P-value of this test were 88.90 and 0.0001, respectively. Rejecting H_o, we concluded that the slopes of the six methods were not equal and that each method required its own slope coefficient when dbh was used as a covariate. We then refit Equation 8 specifying $e_{ijk} \sim N(0, \sigma^2_G)$ or separate residual variance components for the same-face and opposite-face groups (G). Comparing this model versus $e_{ijk} \sim N(0, \sigma^2)$ is a test of $\sigma^2_{Vel\_S} = \sigma^2_{Vel\_O}$ and can be accomplished via a likelihood ratio test, which is asymptotically distributed as χ^2_1. The value of the test statistic, or the differences of twice the negative log-likelihoods, between the full and reduced models was 804.4, with a corresponding P-value of 0.0001, suggesting separate residual errors for the same-face and opposite-face methods.

A plot of the estimated regression lines versus dbh for each method is presented in Figure 3. Figure 3 indicates that velocities are generally higher for the Vel_S, Vel_OA, and Vel_OC methods compared with the Vel_OE, Vel_OD, and Vel_OU methods. Figure 3 also indicates that velocities determined using Vel_S and Vel_OC methods do not vary with increasing dbh. The regression coefficients, corresponding standard errors, P-values, and variance components for the final model are presented in Table 2. Plots of the residuals from the final model indicated no general trends or outliers. In Table 2, the population regression coefficients correspond to β_{0,Vel_S} and β_{1,Vel_S}, and $\beta_{0,Vel\_O\cdot}$ and $\beta_{1,Vel\_O\cdot}$ correspond to deviations from the population parameters. The slope coefficient for Vel_S was not significantly different from zero ($\hat{\beta}_{1,Vel\_S}$; P-value = 0.7842) and suggests that velocity does not depend on dbh when the probes are placed on the same side of the tree or a simple mean model adequately describes velocities for the same-face method.

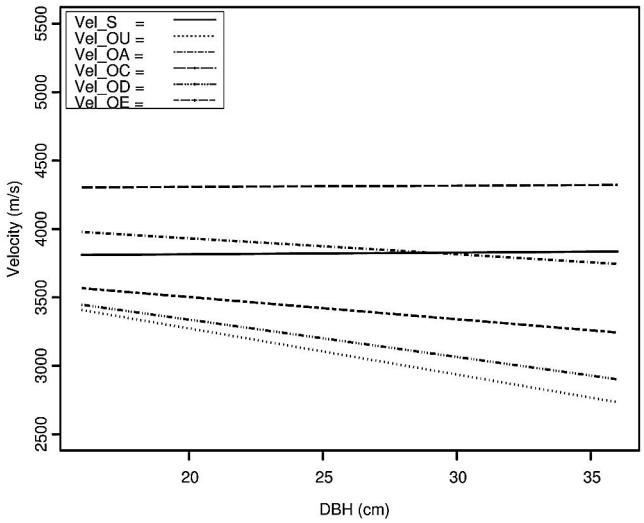

Figure 3. Plot of estimated regression lines for comparing same-face– and opposite-face–determined velocity.

Table 2. Regression coefficients, corresponding standard errors, *P*-values, and variance components for the final model, where β_{0,Vel_S} and β_{1,Vel_S} correspond with the population level parameters, and $\beta_{0,Vel\_O\cdot}$ and $\beta_{1,Vel\_O\cdot}$ correspond with deviations from the population parameters.

Effect	Estimate	Standard Error	DF	t-value	*P*-value
$\hat{\beta}_{0,Vel\_S}$	3789.33	120.22	114	31.52	0.0001
$\hat{\beta}_{0Vel\_OU}$	156.87	48.93	399	3.21	0.0015
$\hat{\beta}_{0Vel\_OA}$	375.61	48.93	399	7.68	0.0001
$\hat{\beta}_{0Vel\_OC}$	500.47	48.93	399	10.23	0.0001
$\hat{\beta}_{0Vel\_OD}$	93.74	48.93	399	1.92	0.0561
$\hat{\beta}_{0Vel\_OE}$	36.42	48.93	399	0.74	0.4571
$\hat{\beta}_{1Vel\_S}$	1.28	4.66	114	0.27	0.7842
$\hat{\beta}_{1Vel\_OU}$	−34.95	1.89	399	−18.44	0.0001
$\hat{\beta}_{1Vel\_OA}$	−12.95	1.89	399	−6.83	0.0001
$\hat{\beta}_{1Vel\_OC}$	−0.39	1.89	399	−0.21	0.8356
$\hat{\beta}_{1Vel\_OD}$	−28.55	1.89	399	−15.06	0.0001
$\hat{\beta}_{1Vel\_OE}$	−17.46	1.89	399	−9.21	0.0001

$\hat{\sigma}^2_t = 44.557$; $\hat{\sigma}^2_{Mt} = 2{,}606.91$; $\hat{\sigma}^2_{Vel\_S} = 42{,}810$; $\hat{\sigma}^2_{Vel\_O\cdot} = 16{,}237$.

The P-values for the estimated slope coefficients of the opposite-face method ($\beta_{1,Vel\_O\cdot}$) given in Table 2, correspond to pairwise comparisons with β_{1,Vel_S}. These results suggest that the slope coefficients of the opposite-face method all differ significantly from β_{1,Vel_S}, with the exception of β_{1,Vel_OC} (Figure 3). In addition, this finding indicates that velocity calculated assuming a circumferential flight path around the stem and then downward to the receiving probe removes the effect of the amount of wood through which the stress wave passes, but Vel_OU, Vel_OA, Vel_OD, and Vel_OE all depend on dbh (Tables 2 and 3). Finally, the similar slope coefficients for the same-face method and the opposite-face method assuming a circumferential flight path suggests that comparing Vel_S with Vel_OC is equivalent to testing the intercepts. The P-value of this test is equivalent to the P-value of the $\hat{\beta}_{0,Vel\_OC}$ parameter estimate and was 0.0001, indicating that the estimate of Vel_OC is significantly larger ($\hat{\beta}_{0,Vel\_OC} = 500.47$) than Vel_S. Table 2 also indicates that Vel_OU, Vel_OA, Vel_OD, and Vel_OE all depend on dbh or the amount of wood through which the stress wave passes. Pairwise comparisons between the opposite-face methods indicate that the slope coefficients all differ significantly from each other,

Table 3. Estimates and *P*-values of pairwise comparisons between the slopes.

Comparison	Estimate	Standard error	*P*-value
$\beta_{1,Vel\_S}-\beta_{1,Vel\_OU}$	34.95	1.89	0.0001
$\beta_{1,Vel\_S}-\beta_{1,Vel\_OA}$	12.95	1.89	0.0001
$\beta_{1,Vel\_S}-\beta_{1,Vel\_OC}$	0.39	1.89	0.8356
$\beta_{1,Vel\_S}-\beta_{1,Vel\_OD}$	28.55	1.89	0.0001
$\beta_{1,Vel\_S}-\beta_{1,Vel\_OE}$	17.46	1.89	0.0001
$\beta_{1,Vel\_OU}-\beta_{1,Vel\_OA}$	−21.99	1.73	0.0001
$\beta_{1,Vel\_OU}-\beta_{1,Vel\_OC}$	−34.55	1.73	0.0001
$\beta_{1,Vel\_OU}-\beta_{1,Vel\_OD}$	−6.40	1.73	0.0003
$\beta_{1,Vel\_OU}-\beta_{1,Vel\_OE}$	−17.49	1.73	0.0001
$\beta_{1,Vel\_OA}-\beta_{1,Vel\_OC}$	−12.55	1.73	0.0001
$\beta_{1,Vel\_OA}-\beta_{1,Vel\_OD}$	15.60	1.73	0.0001
$\beta_{1,Vel\_OA}-\beta_{1,Vel\_OE}$	4.51	1.73	0.0099
$\beta_{1,Vel\_OC}-\beta_{1,Vel\_OD}$	28.15	1.73	0.0001
$\beta_{1,Vel\_OC}-\beta_{1,Vel\_OE}$	17.06	1.73	0.0001
$\beta_{1,Vel\_OD}-\beta_{1,Vel\_OE}$	−11.09	1.73	0.0001

suggesting no similarities among the distance adjusted velocities (Table 3).

Figure 4 is a plot of observed velocities calculated using the same-face and opposite-face methods, estimated regression lines, and corresponding 95% confidence intervals. Figure 4 shows that the estimated values of Vel_S are significantly larger compared with Vel_OU, Vel_OD, and Vel_OE across the range of dbh values. This indicates that these transformations did not adequately account for the amount of wood through which the stress wave passes. Figure 4 also shows no significant differences exist between velocities determined using the Vel_S and Vel_OA methods across the range of dbh values. The estimates of the pairwise slope comparisons versus β_{1,Vel_S} (Table 3) suggest that the order of effectiveness in removing the effect of stem size, from greatest to least, is $\hat{\beta}_{1,Vel\_OC} = 0.39$, $\hat{\beta}_{1,Vel\_OA} = 12.95$, $\hat{\beta}_{1,Vel\_OE} = 17.46$, $\beta_{1,Vel\_OD} = 28.55$, and $\hat{\beta}_{1,Vel\_OU} = 34.95$, respectively.

Plots of observed velocities, estimated regression lines, and corresponding 95% confidence intervals for comparing velocities determined from the opposite-face methods were also examined. These plots indicated that Vel_OC velocities were significantly higher compared with all other opposite-face adjusted velocities. Similarly, velocities from the Vel_OU method were found to be significantly lower compared with all other opposite-face methods, with the exception of the Vel_OD method. Comparing Vel_OU and Vel_OD across the range of dbh values showed no significant difference between these two methods, meaning that within this diameter range, the velocities are equivalent. Comparing Vel_OE with Vel_OU and Vel_OD suggested no significant differences in smaller dbh trees, but these curves began to diverge with increasing dbh.

The variance components in Table 2, indicate that more variation exists between trees ($\hat{\sigma}_t^2 = 44{,}557$) than among methods by tree combinations ($\hat{\sigma}_{Mt}^2 = 2{,}606.91$). The inclusion of tree-level covariates such as total height, height to base live crown, or other tree-specific characteristics could be incorporated to reduce the between-tree variation. The residual errors for the methods clearly show more variation from hit-to-hit using the same-face method with $\hat{\sigma}_{Vel\_S}^2 = 42{,}810$ and residual error values of $\hat{\sigma}_{Vel\_O.}^2 = 16{,}237$ for the opposite-face methods. This suggests that from hit-to-hit, the same-face method was approximately 2.6 times more variable than the opposite-face methods we examined, i.e., from hit-to-hit the opposite face methods were 62% less variable than the same-face method.

Discussion

The results of this analysis suggest significant differences in velocities when the transmitting and receiving probes of an acoustic instrument are placed on the same or opposite faces of a standing tree. These findings generally indicate that velocities, determined using the opposite-face method, depend on the amount of wood or the size of the stem through which the stress wave must pass. However, velocity does not depend on stem size when using the same-face method. These findings are in general agreement with Chauhan and Walker (2006) and Toulmin and Raymond (2007), who found low relationships between acoustic velocity and dbh.

The acoustic velocities for the opposite-face methods were generally slower than the same-face method (Vel_S), with the exception being Vel_OC. One possible explanation for the higher velocities using the Vel_OC method is that TOF was held constant even though the Vel_OC method had a longer flight path than the other methods (Table 2). An inherent assumption of the Vel_OC method is that the stress wave travels around the stem faster than it does longitudinally; however, Bucur (2006) reports that ultrasonic velocities are much higher (approximately an order of magnitude) in the longitudinal direction (fiber direction) than the radial or tangential direction.

We also found that the variation of velocities from hit-to-hit was 62% less using the opposite-face method versus the same-face method. The reason for this finding is unclear but may potentially be attributed to the physiological formation of the wood through which the stress wave passes through.

Several different flight paths for the opposite-face method were investigated in this work, and of those, the Vel_OC method was the only method that removed the effect of stem size, presumably because it includes the circumference of the tree in its determination. However, numerous alternative flight paths are possible and may provide results similar to the Vel_OC method. For example, given that the stress wave prefers to travel in high stiffness (mature) wood, another potential path is possible that involves the stress wave traveling from the transmitting probe radially through the mature wood to the juvenile core, around the circumference of the juvenile core, and then radially through the mature wood again on the opposite side of the tree, and then down longitudinally to the receiving probe. This potential flight path is a combination of the Vel_OA (across the stem then down) and Vel_OC (circumferentially around the stem in the mature wood then down) methods. The distance traveled assuming this flight path would be larger than those calculated using the Vel_OA (average distance of 1.25 m) method and smaller than those calculated using the Vel_OC method (average distance of 1.40 m). The combination of the Vel_OA and Vel_OC methods could potentially remove the effect of stem size observed with the Vel_OA method. This transformation would also yield lower velocities than those observed using the Vel_OC method, because for fixed time, decreasing the distance traveled will result in a lower velocity.

Researchers who attempt to calculate stress wave–determined MOE from acoustic tools and green density may not be accurate in their estimate if the opposite-face method is used and velocities are not adjusted accordingly. If density is held constant, and velocity is not adjusted for the distance the stress wave travels, and then dynamic MOE will be underestimated as stem size increases. Similarly, if velocity is unadjusted and a whole core or average stem density is

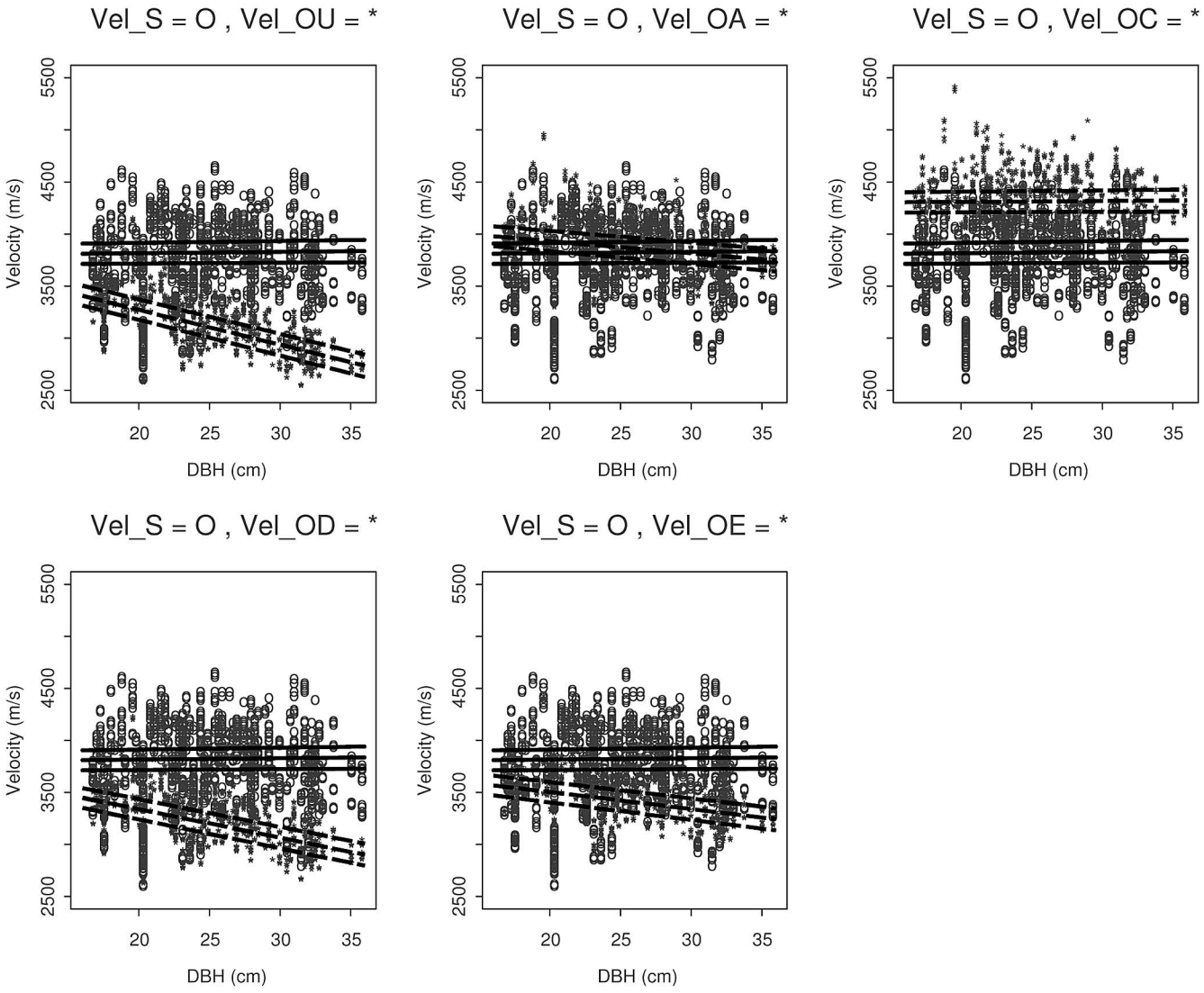

Figure 4. Plot of observed velocities, estimated regression lines (○ = ——; * = - - - - -) and corresponding 95% confidence intervals, for comparing same-face– and opposite-face–determined velocity.

used, then dynamic MOE will again be underestimated, and attempting to correlate a whole-tree average for machine graded MOE based on cut boards could lead to erroneous results. This may explain the low correlations observed by Matheson et al. (2002), when they correlated unadjusted velocity measured on standing trees with a whole-tree average for board stiffness.

Preliminary results from a current study being conducted by the authors show that the Vel_OC and Vel_S flight paths outperform the Vel_OA, Vel_OD, Vel_OE, and Vel_OU flight paths when correlated with whole-tree averaged stress graded MOE with *R* values of 0.71 and 0.70, respectively. These correlations show both calculations could be used to predict whole-tree averaged MOE reasonably well. Because the opposite-face method is 62% less variable from hit-to-hit, it is recommended to use the Vel_C opposite-face method when calculating standing tree velocities.

Conclusions

Comparison of acoustic velocities measured using transmitting and receiving probes placed on the same face and opposite faces for 100 standing loblolly pine (*Pinus taeda*) trees, showed significant differences in velocity between the two methods. Velocity determined using the opposite-face method generally depended on stem size or the amount of wood through which the stress wave must pass. For the opposite-face method five possible flight paths were examined and the only opposite-face method in which its velocities did not vary with dbh was for an assumed flight path where the stress wave traveled from the transmitting probe around the circumference of the stem in the outerwood and then down longitudinally to the receiving probe. Variation in velocities from hit-to-hit was 62% less using the opposite-face method compared with the same-face method. It is recommended to use the circumferential opposite-face (Vel_OC) calculation when determining stress wave velocity for a standing tree.

Literature Cited

BOOKER, R., AND RIDOUTT, B.G. 1997. *Stiffness testing of standing trees*. FRI Bull. 202.

BORDERS, B.E., R.E. WILL, D. MARKEWITZ, A. CLARK, III, R. HENDRICK, R.O. TESKEY, AND Y. ZHANG. 2004. Effect of complete competition control and annual fertilization on stem growth and canopy relations for a chronosequence of loblolly pine plantations in the lower coastal plain of Georgia. *For. Ecol. Manag.* 192:21–37.

BUCUR, V. 2006. *Acoustics of wood*, 2nd Ed. Springer-Verlag, Berlin Heidelberg, New York. 400 p.

CARTER, P.C.S., AND N.J. SHARPLIN (INVENTORS). 2006. *Timber harvesting apparatus*. International Patent WO/2006/049514, Nov. 11, 2006.

CHAUHAN, S.S., AND J.C.F. WALKER. 2006. Variations in acoustic velocity and density with age, and their interrelationships in radiata pine. *For. Ecol. Manag.* 229:388–394.

GRABIANOWSKI, M., B. MANLEY, AND J.C.F. WALKER. 2006. Acoustic measurements on standing trees, logs, and green lumber. *Wood Sci. Technol.* 40:205–216.

JOE, B., R. DICKSON, C. RAYMOND, J. ILIC, AND C. MATHESON. 2004. *Prediction of Eucalyptus dunnii and Pinus radiata timber stiffness using acoustics.* RIRDC Publ. 04/013. 121 p.

LINDSTROM, H., P. HARRIS, AND R. NAKADA. 2002. Methods for measuring stiffness of young trees. *Holz Roh Werkst.* 60:165–174.

MATHESON, A.C., R.L. DICKSON, D.J. SPENCER, B. JOE, AND J. ILIC. 2002. Acoustic segregation of *Pinus radiata* logs according to stiffness. *Ann. For. Sci.* 59: 471–477.

SAS INSTITUTE, INC. 2004. *SAS 9.1.3 Help and documentation*. SAS Institute, Inc., Cary, NC.

TOULMIN, M.J., AND C.A. RAYMOND. 2007. Developing a sampling strategy for measuring acoustic velocity in standing *Pinus radiata* using the treetap time of flight tool. *N.Z. J. For. Sci.* 37(1):96–111.

WANG, X., R.J. ROSS, M. MCCLELLAN, R.J. BARBOUR, J.R. ERICKSON, J.W. FORSMAN, AND G.D. MCGINNIS. 2001. Nondestructive evaluation of standing trees with a stress wave method. *J. Wood Fiber Sci.* 33(4):522–533.

WANG, X., R.J. ROSS, AND P. CARTER. 2007. Acoustic evaluation of wood quality in standing trees. Part I. Acoustic wave behavior. *J. Wood Fiber Sci.* 39(1):28–38.